
Figures and figure supplements

Positively selected modifications in the pore of TbAQP2 allow pentamidine to enter *Trypanosoma brucei*

Ali H Alghamdi et al

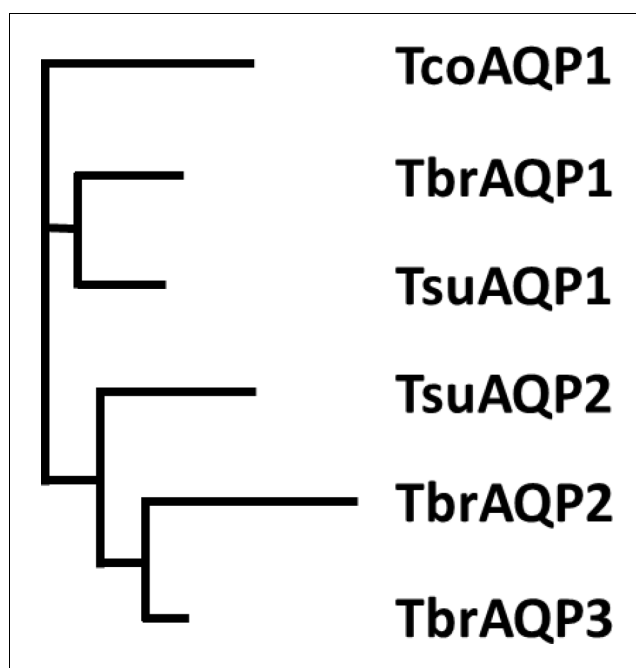


Figure 1. Phylogenetic tree of *Trypanosoma* aquaporins. The tree is a Neighbour-joining tree produced in Clustal Omega with the lengths of the horizontals proportional to the differences.

Tco	MTSPTVPNPMSTVPMTEM---TE-ANGTTNPPIPDAGERTAV---NFDTEQCK-TKEIL	51
Tbr1	MSD--EKINVHQYPSSETDVRGLKARNGGACEVPFEENN-EPIPNRSANPQEKNE--NELV	55
Tsu1	MSS--EPVNVHRYTAEGDRSGLKDRHGKTCEVCVGDESAAAVPSAVYNPQEQQSGDGPEVK	58
Tsu2	MQN--QPDAMTH-STAVQMV-NKNPEDGTGGADTERSEMTAP-----TTRTGDAQK	48
Tbr2	MQS--QPDNVAY-PMELQAV-NKDGT---VEVRVQGNVDNNSN-----ERWDADVQK	45
Tbr3	MQS--QPDNVAY-PMELQAV-NKDGT---VEVRVQGNDDSS-----NRK	37
	* . : .	
Tco	-AGEGEAPHGPMDINYWPLRLNLRMDFREYVGEFLGTFVLLFMGNGVVATTLLDNNLGFLS	110
Tbr1	GDNADNEAHDADVNYWAPRQLRLDYRNYMGFEFLGTFVLLFMGNGVVATTILDKDLGFLS	115
Tsu1	AGGGEAEVQNAADVNNWAPRRLRLDYRDYMGFEFLGTFVLLFMGNGVVATTMLDDGLGFLS	118
Tsu2	CETTNTPKEGAGGINYWAPRELRLKYRDYMGELLGTFVLLLMGNGVVATVVVDGKLGFLS	108
Tbr2	HEVAEAQEKPVGGINFWAPRELRLNYRDYVAEFLGNFVLIYIAKGAVITSLVPDFGLLG	105
Tbr3	HEVAEAQEEVPGGINFWAPRELRLNYRDYMGELLGTFVLLFMGNGVVATVIIDGKLGFLS	97
	. : * * * . * : : * : : * : * : * : : * : * : * : : * : * : *	
Tco	ITFGWGIAVTMGLYVSLGTSSGHLNPAVTVANAFFGGFPWKKVPGYIAMQMLGAFVGAAC	170
Tbr1	ITLGGWGIAVTMGLYISLGTSCGHLNPAVTLANAVFGCFPWRRVPGYIAAQMLGAFVGAAC	175
Tsu1	ITLGGWGIAVTMGLYISLGTSCGHLNPAVTVANAVFGCFPWKKVAGYIAMQMLGAFVGAAC	178
Tsu2	ITLGGWGIAVTMALYISLGTSSGHLNPAVTVGNVAVFGDFPWRKVPGYIAAQMFAGFLGAAC	168
Tbr2	LTIGIGVAVTMALYVSLGTSSGHLNSAVTVGNVAVFGDFPWRKVPGYIAAQMLGTFGLGAAC	165
Tbr3	ITLGGWGIAVTMALYVSLGTSSGHLNPAVTVGNVAVFGDFPWRKVPGYIAAQMLGAFGLGAAC	157
	: * : * : * : * : * : * : * : * : * : * : * : * : * : * : * : * : * : *	
Tco	AYGVYADLLNKKVSDG---EIEDYAGMFSTYPRDGNLSLFCIFGEFICTAMLTFCVCGI	226
Tbr1	AYGVYADLLKQHSYG-LVGFQDKGFAGMFSTYPRGNRLFYCIFSEFICTAILLFCVGGI	234
Tsu1	AYGVFADLLKQHSYG-LIPFGDKGFAGMFSTYPRDGNRLFYCIFGEFICTAMLLFCVSGI	237
Tsu2	AYGVFADLLKEYCGGKLLAFGAKGIAGVFSTYKEANSVFACVFGEFICTAILLFCVCGI	228
Tbr2	AYGVFADLLKAHGGGELIAFGEKGIWVFAMYPAEENGIFYPIFAELISTAVLLLCVCGI	225
Tbr3	AYGVFADLLKAHGGGELIAFGEKGTAGVFSTYPRDSNGLFSCIFGEFICTAMLLFCVCGI	217
	*** : *** : . . : . * : * : * : * : * : * : * : * : * : * : * : *	
Tco	FDTHNAPATGHEPLAVGALVFAIGNNVGYATGYA INPARDFGPRVFSAILYGSTVFTRGD	286
Tbr1	FDPNNSPAKGHEPLAVGALVFAIGNNIGYASGYA INPARDFGPRVFSAILFGSEVFTTGN	294
Tsu1	FDANNSPAKGHEPLAVGALVFAIGNNIGYATGYA INPARDFGPRVFSAILFGSEVFTAGN	297
Tsu2	FDPNNSPAKKHEPLAVGSLIFAIGNNIGYSTGYAMNPARDFAPRVFSALLLGGEVFSHGN	288
Tbr2	FDPNNSPAKGYETVAIGALVFVMVNNFGLASPLAMNPSLDFGPRVFGAILLGGEVFSHAN	285
Tbr3	FDPNNSPAKGHEPLAVGALVFAIGNNIGYSTGYA INPARDFGPRVFSFLYGGKVFSHAN	277
	* * : * : * : * : * : * : * : * : * : * : * : * : * : * : * : * : * : *	
Tco	YYFWVPLFIPLLGIFGIILYKYFVPH	313
Tbr1	YYFWVPLFIPFLGGIFGLFLYKYFVPY	321
Tsu1	YYFWVPLFIPFLGGIFGLLLYKYFVPH	324
Tsu2	YYFWVPLFIPFLGAIFGLFLYKYFVPH	315
Tbr2	YYFWVPLVVPFFGAILGLFLYKYFVPH	312
Tbr3	YYFWVPLVIPLFGGIFGLFLYKYFVPH	304
	***** : * : * : * : * : * : * : * : * : * : * : * : * : * : * : *	

Figure 1—figure supplement 1. Sequence alignment and individual sequences of the *T. congolense*, *T. b. brucei* and *T. suis*. The *T. brucei* and *T. congolense* sequences were obtained from tritrypDB, *T. suis* sequences (Kelly S, Gibson W and Carrington M. The genome of *Trypanosoma suis*. In preparation). The alignment was produced with Clustal Omega. The yellow highlighting indicates the N-terminus of the sequences used to determine non-synonymous v synonymous ratios. dN/dS. T brucei AQP1 v T. suis AQP1 0.21. T brucei AQP3 v T. suis AQP3 0.30. T brucei AQP2 v *T. brucei* AQP3 2.00.

```

>Tco AQP1
MTSPTVPNPMSTVPMTEMEANGTTNPPIPDA GERTAVNFDTEQCKTKEILAGEGEAPHGPM DINYWPLRNL RMD
FREYVGEFLGT FVLLFMGNGVVATTLLDNNLGFLSITFGWGIAVTMGLYVSLGTSSGHLNPAVTVANAFFGGFPW
KKVPGYIAMQMLGAFVGAACAYGVYADLLNKKVSDGEIEDYAGMFSTYPRDGNSLFS CIFGEFICTAMLTFCVCG
IFDTHNAPATGHEPLAVGALVFAIGNNVGYATGYAINPARDFGPRVFSAILYGSTVFTRGDYFWVPLFIPLLGG
IFGIILYKYFVPH

>Tbr AQP1
MSDEKINVHQYPSETDVRGLKARNGGACEVPFEENNEPIPNRSANPQEKNE NELVGDNADNEAHDAVDVNYWAPR
QLRLDYRNYMGEFLGT FVLLFMGNGVVATTILDKDLGFLSITLGWGIAVTMGLYISLGISGHLNPAVTLANAVF
GCFPWRRVPGYIAAQMLGAFVGAACAYGVYADLLKQHSGGLVGF GDKGFAGMFSTYPREGNRLFYCIFSEFICTA
ILLFCVGGIFDPNNSPAKGHEPLAVGALVFAIGNNIGYASGYAINPARDFGPRVFSAILFGSEVFTTGNYFWVP
LFIPFLGGIFGLFLYKYFVPY

>Tbr AQP2
MQSQPDNVAYPMELQAVNKDGTVEVRVQGNVDNSSNERWDADVQKHEVAEAEQEKPVGGINFWAPRELRLNYRDYV
AEFLGNFVLIYIAKGA VITSLLPDFGLLGLTIGIGVAVTMALYVSLGISGGHLNSAVTVGNAVFGDFPWRKVP
YIAAQMLGTFLGAACAYGVFADLLKAHGGELIAFGEKGIWVFAMYP AEGNGIFYPIFAELISTAVLLLCVCGI
FDPNNSPAKGYETVAIGALVFMVN NFGLASPLAMNPSLDFGPRVFGAILLGGEVFSHANYFWVPLVVPFFGAI
LGLFLYKYFLPH

>Tbr AQP3
MQSQPDNVAYPMELQAVNKDGTVEVRVQGNDDSSNRKHEVAEAEQEEVPGGINFWAPRELRLNYRDYMGELLGT FV
LLFMGNGVVATV IIDGKLGFLSITLGWGIAVTMALYVSLGISSGHLNPAVTVGNAVFGDFPWRKVPGYIAAQMLG
AFLGAACAYGVFADLLKAHGGELIAFGEKGTAGVFSTYPRDSNGLFS CIFGEFICTAMLLFCVCGIFDPNNSPA
KGHEPLAVGALVFAIGNNIGYSTGYAINPARDFGPRVFSFLYGGKVFSHANYFWVPLVIPFLGGIFGLFLYKY
FVPH

>Tsu AQP1
MSSEPVNVHRYTAEGDRSGLKDRHGKTCEVCVGDESAAVPSAVYNPQE QSGDGPEVKAGGGEAEVQNAADVNNW
APRRLRLDYRDYMG EFLGT FVLLFMGNGVVATTMLDDGLGFLSITLGWGIAVTMGLYISLGTSCGHLNPAVTVAN
AVFGCFPWKKVAGYIAMQMLGAFVGAACAYGVFADLLKQHSGGLIPFGDKGFAGMFSTYPRDGNRLFYCIFGEFI
CTAMLLFCVSGIFDANN SPAKGHEPLAVGALVFAIGNNIGYATGYAINPARDFGPRLFSAILFGSEVFTAGNYFF
WVPLFIPFLGGIFGLLLYKYFVPH

>Tsu AQP2
MQNQPDAMTHSTAVQM VNKNPEDGTGGADTERSDEMTAPTTRTGDAQKCETTNTPK EGAGGINYWAPRELRLKYR
DYMGE LLGT FVLLLMGNGVVATVVVDGKLGFLSITLGWGIAVTMALYISLGISGHLNPAVTVGNAVFGDFPWRK
VPGYIAAQMF GAFLGAACAYGVFADLLKEYCGGKLLAFGAKGIAGVFSTYPKEANSVFACVFGEFICTAILLFCV
CGIFDPNNSPAKKHEPLAVGSLIFAIGNNIGYSTGYAMNPARDFAPRVFSALLLGGEVFSHGNYFWVPLFIPFL
GAIFGLFLYKYFVPH

```

Figure 1—figure supplement 2. The ratio of non-synonymous v synonymous (dN/dS) codon changes calculated for selected comparisons between *T. brucei* and *T. suis* AQPs. The ratios were calculated using a region of high confidence alignments from ~amino acid 60 (highlighted in **Figure 1—figure supplement 1**) to the C-terminus.

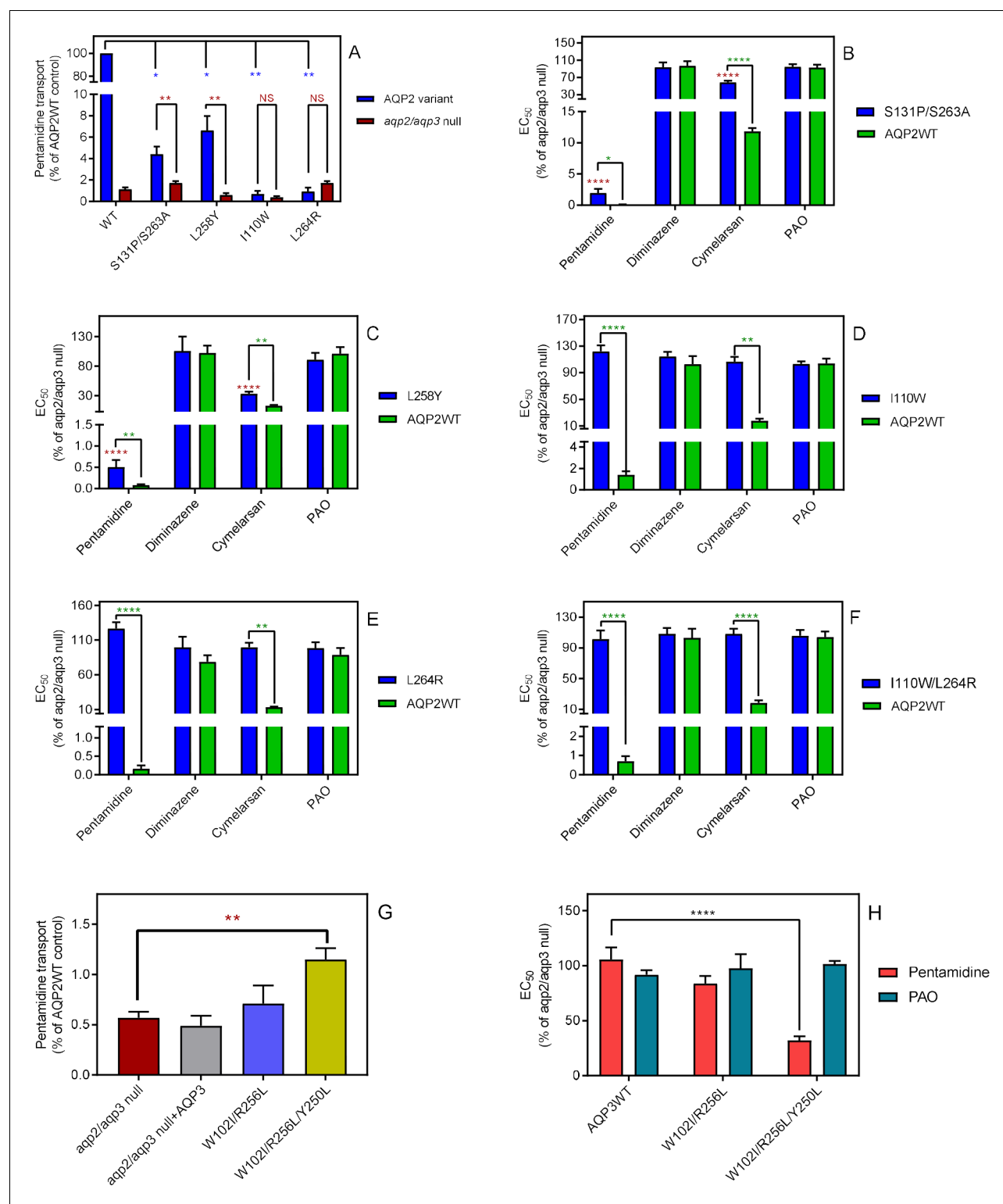


Figure 2. The selectivity filter differences between TbAQP2 and TbAQP3 are largely responsible for their differences in pentamidine sensitivity and transport rates. (A) Transport of 30 nM [³H]-pentamidine by *tbaqp2/aqp3* null cells expressing TbAQP2-WT or one of the TbAQP2 mutants as indicated (blue bars). The corresponding brown bars are pentamidine transport in the control *tbaqp2/aqp3* null cells assessed in parallel in each experiment. Transport was determined in the presence of 1 mM adenosine to block the TbAT1/P2 transporter. Bars represent the average and SEM of at least three independent experiments, each performed in triplicate. Blue stars: statistical significance comparison, by two-tailed unpaired Student's tests, between the cells expressing TbAQP2WT and mutants; red stars: statistical comparison between the AQP2-expressing cells and control cells; NS, not significant. Figure 2 continued on next page

Figure 2 continued

(B–F) EC₅₀ values indicated test drugs, expressed as a percentage of the resistant control (*tbaqp2/tbaqp3* null), against cell lines either expressing the indicated TbAQP2 mutant or TbAQP2WT (sensitive control). Red stars and green stars: comparison with *tbaqp2/aqp3* null or TbAQP2WT-expressing cells, respectively, which were always assessed in parallel in each experiment. (G) Transport of 30 nM [³H]-pentamidine by *tbaqp2/aqp3* null cells expressing TbAQP3 or an AQP3 mutant as indicated. (H) EC₅₀ values of the indicated drugs against *tbaqp2/aqp3* null cells expressing either TbAQP3 or a mutant thereof, expressed as percentage of *tbaqp2/aqp3* null. All data for these graphs are contained in **Figure 2—source data 1**. All experiments are the average and SEM of at least three independent experiments. *, p<0.05; **, p<0.01; ***, p<0.001, ****, p<0.0001 by unpaired Student's t-test, two-tailed.

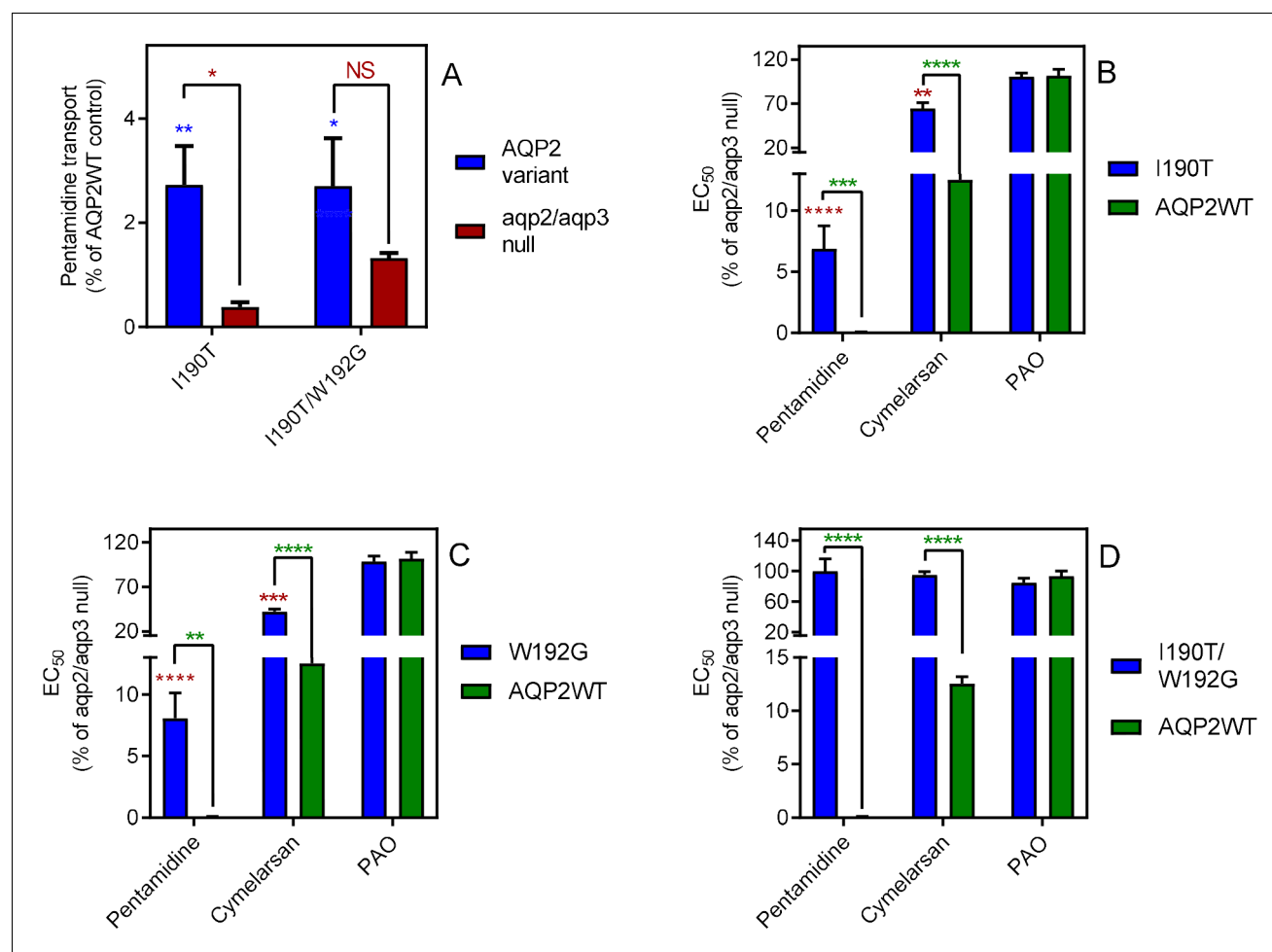


Figure 3. Mutational analysis of TbAQP2 residues I190 and W192. (A) Transport of 30 nM [³H]-pentamidine by *tbaqp2/tbaqp3* null cells or TbAQP2 variants expressed therein. Transport was expressed as a percentage of the rate of the AQP2WT control, performed in parallel. Blue stars are comparison with TbAQP2WT, red stars, comparison with the *tbaqp2/tbaqp3* null control. NS, not significant. (B) EC₅₀ values for the indicated drugs against *tbaqp2/tbaqp3* null cells, and against TbAQP2WT and TbAQP2^{I190T} expressed therein; values were expressed as % of the *tbaqp2/tbaqp3* null (resistant) control. Red stars, comparison with the resistant control; green stars, comparison with the internal sensitive control (TbAQP2WT). The assays for all three strains and all three drugs were done simultaneously on at least three different occasions. (C) As B but for TbAQP2^{W192G}. (D) As B but for TbAQP2^{I190T/W192G}. All data for these graphs are contained in **Figure 3—source data 1**. *, $p < 0.05$; **, $p < 0.01$; ***, $p < 0.001$; ****, $p < 0.0001$ by unpaired Student's t-test.

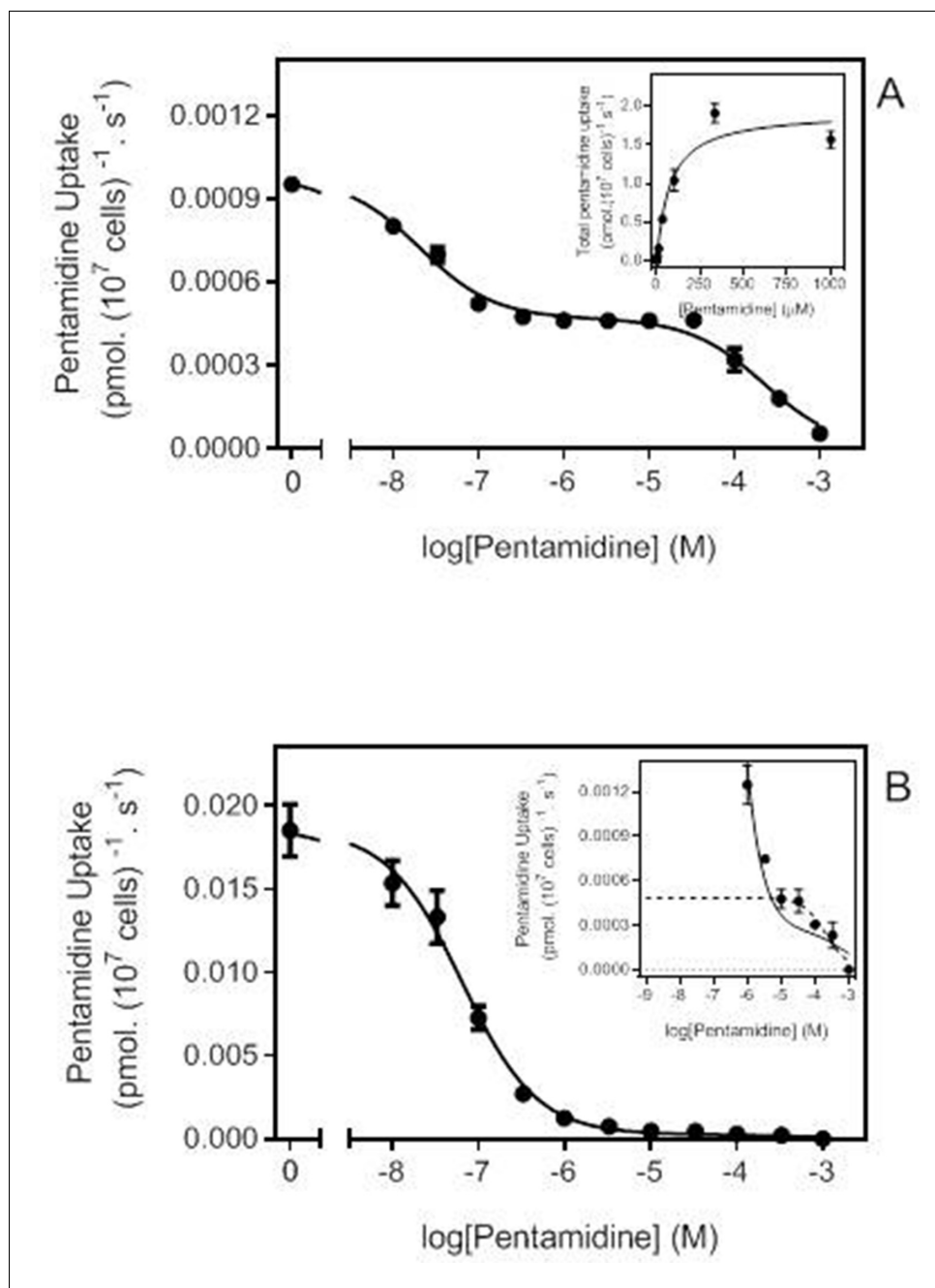


Figure 3—figure supplement 1. Pentamidine transport analysis for TbAQP2^{I190T} and TbAQP2WT. (A) Transport of 30 nM [³H]-pentamidine by *tbaqp2/tbaqp3* null cells expressing TbAQP2^{I190T}, in the presence of unlabelled pentamidine at the indicated concentrations. Incubation time was 15 min, required to ensure sufficient radiolabel for accurate quantification, and uptake was linear and through zero over this period. The inhibition data were plotted to a double sigmoidal curve (Prism 7.0) with the bottom value fixed at 0. The high affinity component displayed an average an IC₅₀ of 30.9 ± 12.2 nM (n = 3) and the lower affinity segment could be converted to a Michaelis-Menten plot for determination of K_m and V_{max} (inset), yielding an average K_m of 59.9 ± 9.1 μM (n = 3), consistent with the Low Affinity Pentamidine Transporter (LAPT1; Bridges et al., 2007). The plot shown is one representative experiment in triplicate of three independent experiments. (B) Like (A) but with *tbaqp2/tbaqp3* null cells expressing TbAQP2WT. Incubation time was 20 s (linear phase). The high affinity phase had statistically identical EC₅₀ (41 ± 17 nM; p>0.05) as TbAQP2^{I190T}. The inset shows a zoom-in on the low-affinity part of the curve (LAPT1 contribution), with the dotted line representing a theoretical sigmoid plot for one inhibitor, with the upper limit fixed at the value obtained for 10 μM pentamidine. The low affinity component was also statistically identical

Figure 3—figure supplement 1 continued on next page

Figure 3—figure supplement 1 continued

in the two strains (TbAQP2-WT $K_m = 82.7 \pm 17.5 \mu\text{M}$ ($n = 3$; $p > 0.05$)). Note that the amount of [^3H]-pentamidine taken up by the low affinity component is highly similar for the mutant (A) and control (B) cell lines, at approximately $0.0005 \text{ pmol}(10^7 \text{ cells})^{-1} \text{ s}^{-1}$. Both frames show one representative experiment of three repeats, each performed in triplicate. Error bars are SEM, when not shown, fall within the symbol. All data for these graphs are contained in **Figure 3—source data 1**.

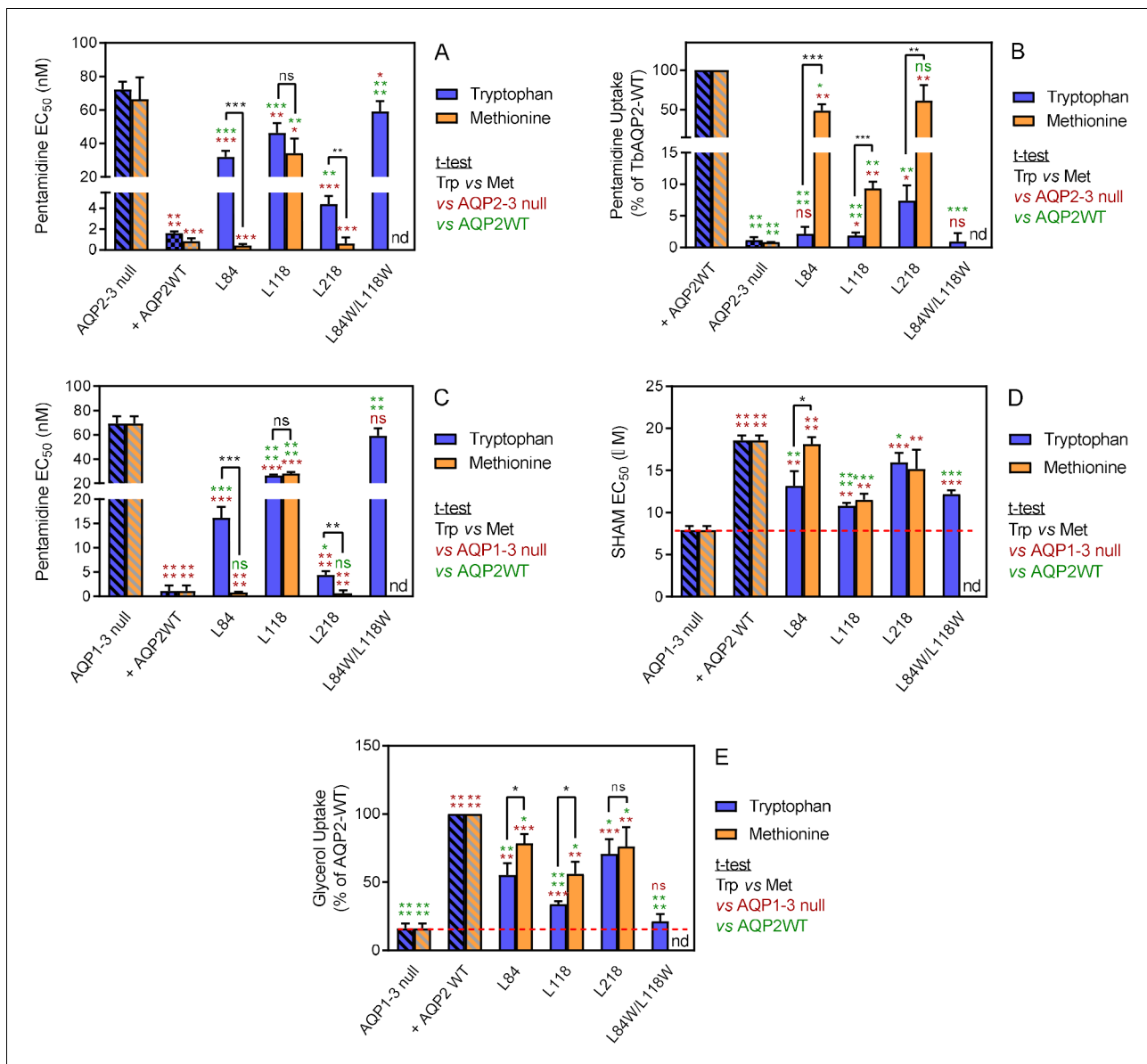


Figure 4. Analysis of TbAQP2 variants with a leucine-to-tryptophan or leucine-to-methionine substitution near the cytoplasmic end of the pore. (A) Pentamidine EC₅₀ values (nM) for mutant and WT TbAQP2 expressed in *tbaqp2/tbaqp3* cells (*aqp2-3* null). The mutants are either a Trp (dark blue bars) or Met (orange bars) substitution at the indicated positions. The resistant control (*aqp2-3* null) and sensitive control (AQP2WT) for the separate datasets (Trp or Met) are indicated as hatched bars in the same colours. (B) As (A) but showing transport of 30 nM [³H]-pentamidine by the same cell lines, expressed as percentage of the transport rate in the TbAQP2 control cells. (C) Pentamidine EC₅₀ values for the same mutants as in (A) but expressed in the *tbaqp1-2-3* null cells, performed in parallel with the determination of EC₅₀ values for SHAM, shown in (D). As all cell lines were done simultaneously, the resistant and sensitive strain control values are identical for the Trp and Met mutants in this series. All bars represent the average and SEM of at least three independent replicates. *, *p*<0.05; **, *p*<0.01; ***, *p*<0.001, ****, *p*<0.0001 by unpaired Student's *t*-test; ns, not significant; nd, not determined. All data for these graphs are contained in **Figure 4—source data 1**.

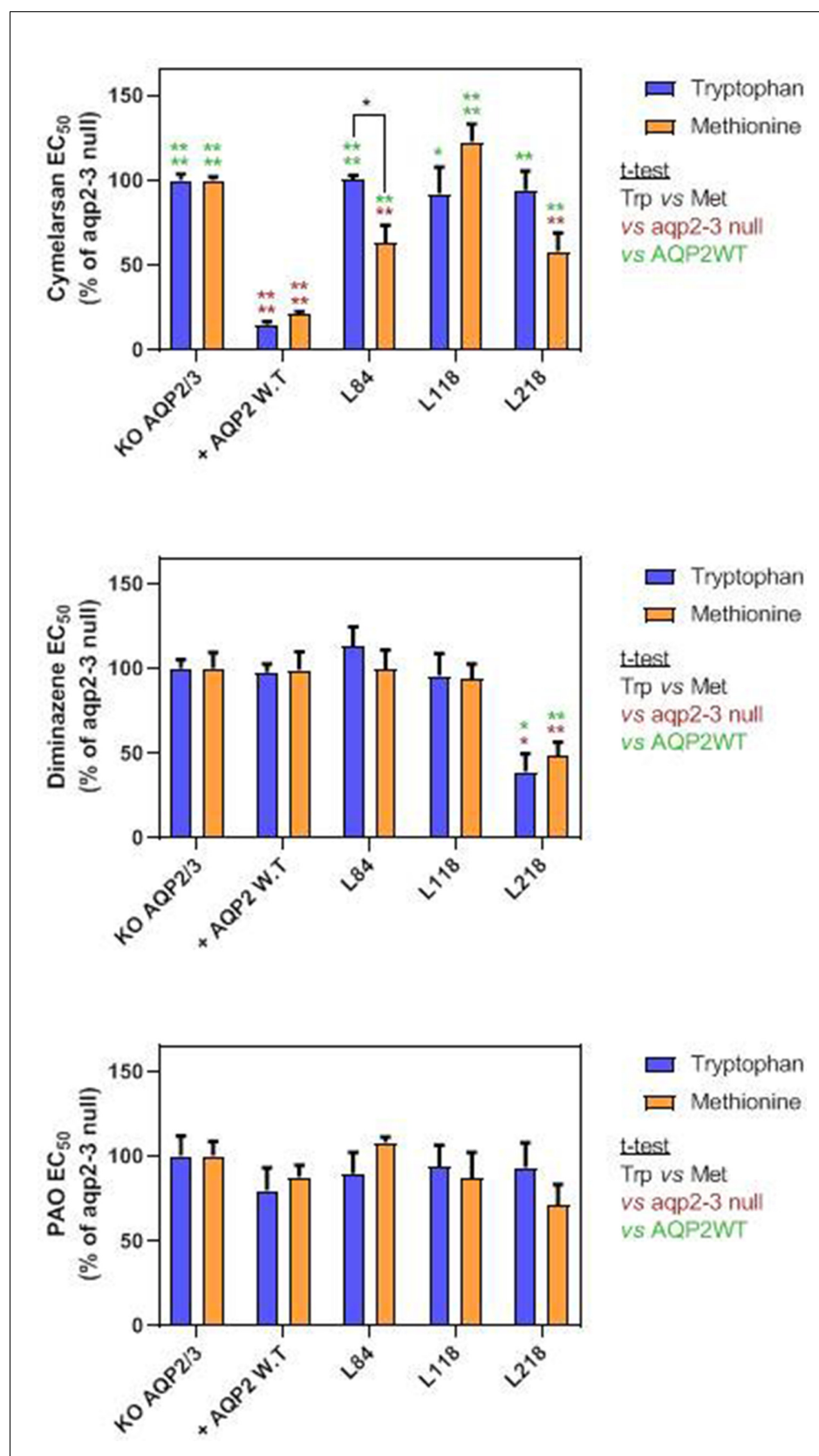


Figure 4—figure supplement 1. EC₅₀ values for Cymelarsan, diminazene acetate and phenylarsine oxide (PAO) against the *tbaqp2-tbaqp3* null cell line. AQP2-WT and various mutant versions thereof (indicated) were expressed

Figure 4—figure supplement 1 continued on next page

Figure 4—figure supplement 1 continued

in this cell line. EC₅₀ values were determined using the alamar blue (resazurin) assay. Bars represent the average and SEM for at least three determinations. nd, not done. All data for these graphs are contained in **Figure 4—source data 1**.

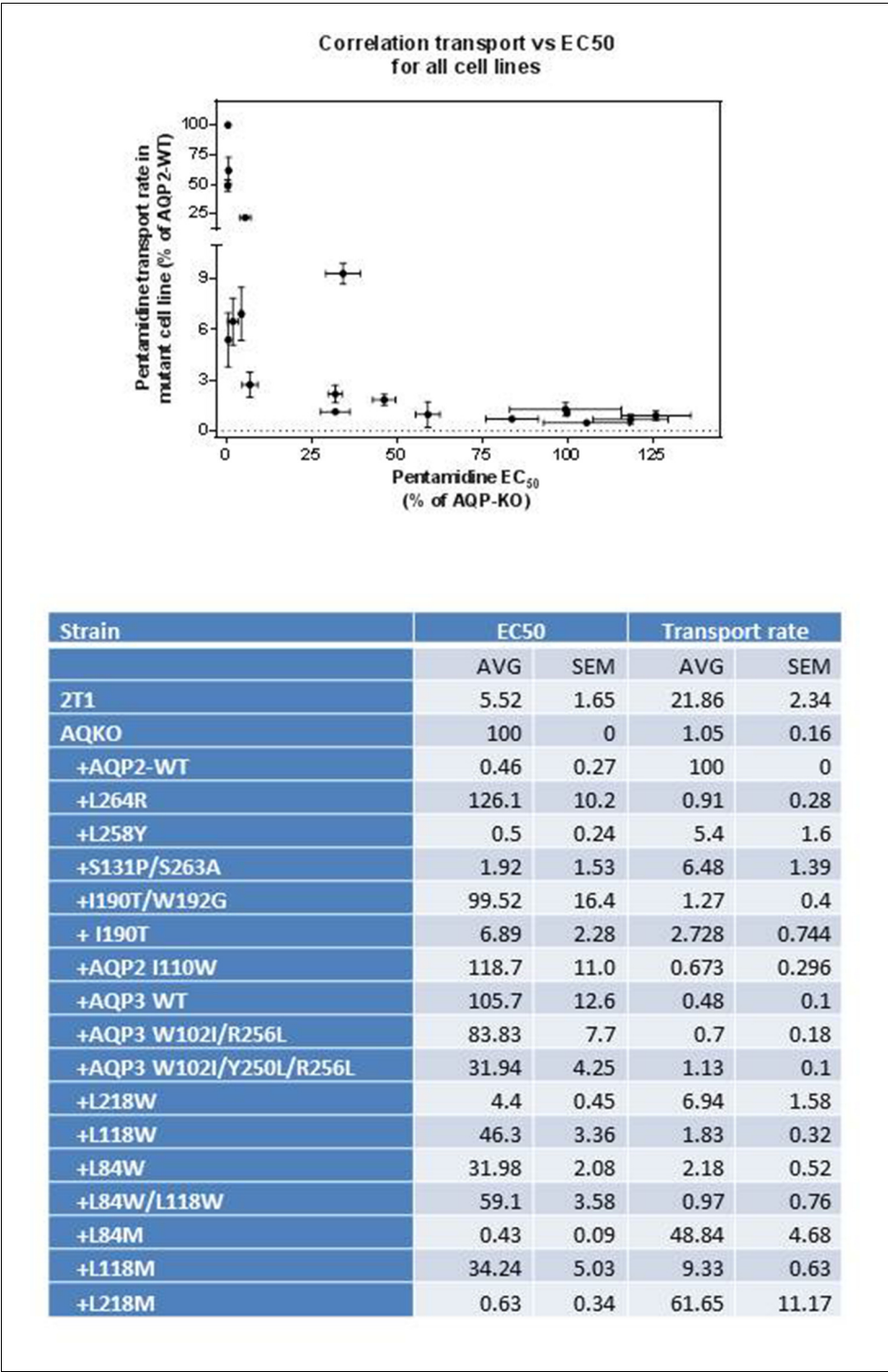


Figure 4—figure supplement 2. Correlation of the EC₅₀ value with the rate of pentamidine transport for all 19 cell lines expressing a wild-type or mutant TbAQP2 in the *aqp2/3* null *T. b. brucei* line. All EC₅₀ values are expressed as percentage of the resistant control, *aqp2/3* null transfected with an empty vector (no TbAQP2). 2T1 is the parental cell line of the *aqp2/3* null. All values are the average of at least three independent determinations; the sensitive and resistant control cell lines were included in each independent experiment and the percentages taken are from the internal control rather than from the grand average over all experiments. All data for these graphs are contained in **Figure 4—source data 1**.

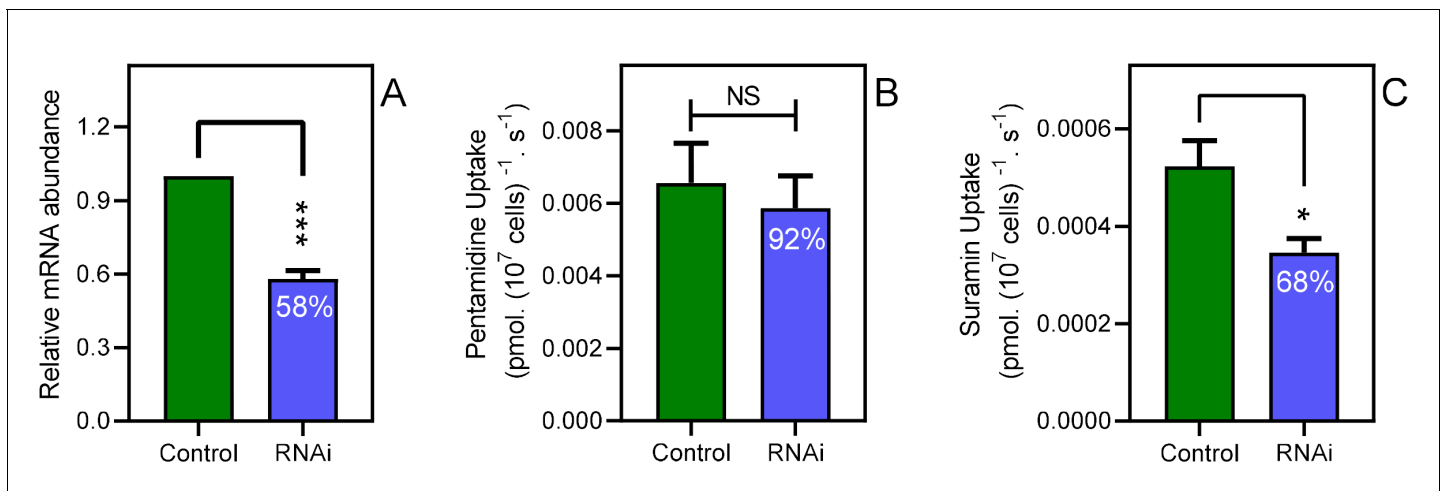


Figure 5. Disabling endocytosis does not reduce uptake of pentamidine. (A) qRT-PCR of CRK12, normalised to housekeeping gene GPI-8 ($n = 3$). (B) Transport of $0.025 \mu\text{M}$ [^3H]-Pentamidine measured in control (non-induced) and CRK12 cell after exactly 12 hr of tetracycline induction; incubation time with label was 30 s. Bar is average and SEM of 5 independent determinations, each performed in triplicate. NS, not significant by unpaired Student's t -test. (C) As frame B but uptake of $0.25 \mu\text{M}$ [^3H]-suramin over 15 min; average and SEM of 5 independent determinations, each in quadruplicate. **, $p=0.0027$ by Student's unpaired, two-tailed t -test. All data for these graphs are contained in **Figure 5—source data 1**.

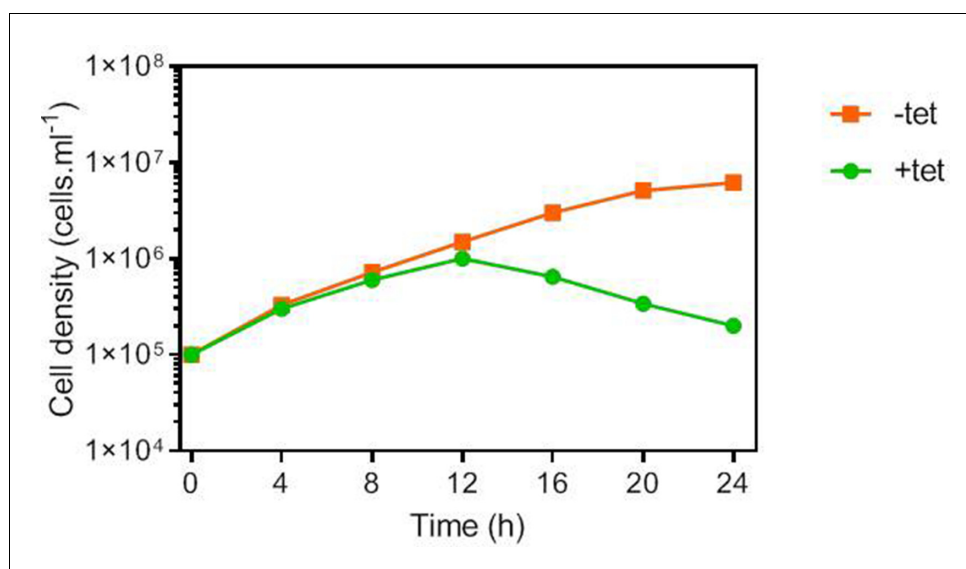


Figure 5—figure supplement 1. Growth Curve of CRK12 RNAi cells in full HMI-9 medium at 37°C/5% CO₂, in the presence or absence of 1 µg/ml tetracycline (tet). Cell counts were performed with a haemocytometer and the average of duplicate determinations is shown. All data for these graphs are contained in **Figure 5—source data 1**.

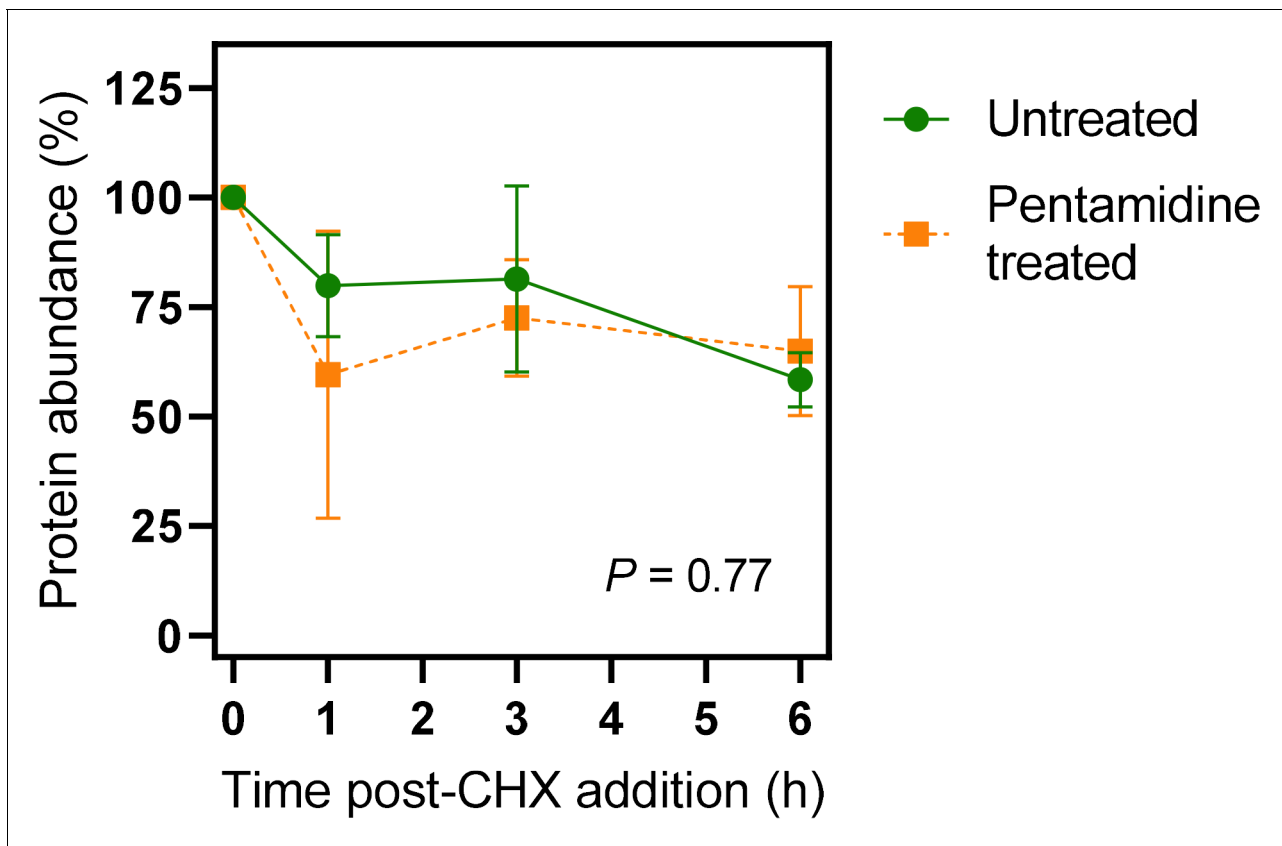


Figure 6. Quantification of western blots of ^{3}H A-TbAQP2. Cells were induced for expression of ^{3}H A-TbAQP2, pretreated with cyclohexidine and subsequently with 25 nM pentamidine ($5\times \text{EC}_{50}$). Western blots (**Figure 6—figure supplement 1**) were performed using anti-HA antiserum in order to quantify the relative amount of TbAQP2 in the cells. The two datasets were not significantly different by Kolmogorov-Smirnov test ($p=0.77$) and data points at each time point were also not significantly different by Student's t-test ($p>0.05$). All data for these graphs are contained in **Figure 6—source data 1**.

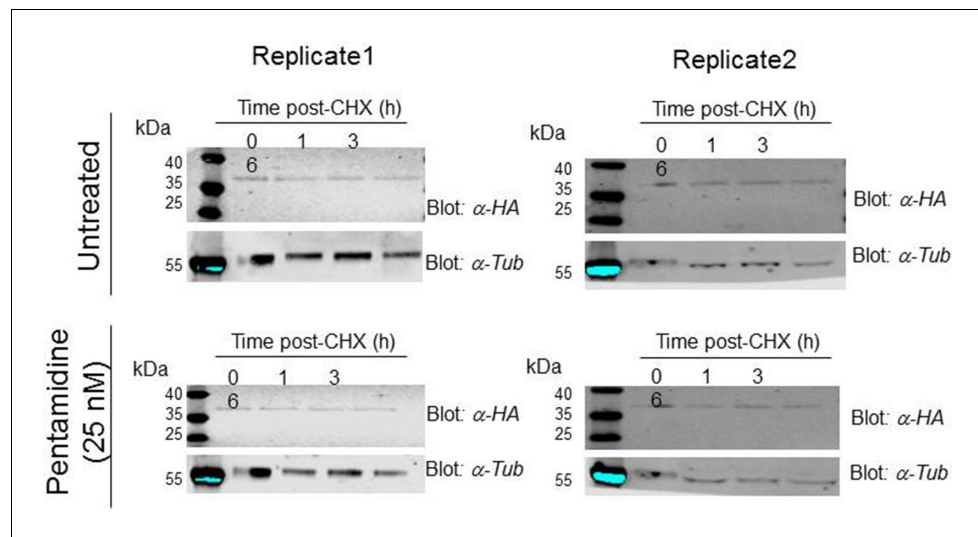


Figure 6—figure supplement 1. Western blots for a $3\times\text{HA}$ AQP2 turnover assay in untreated *T. brucei* 2T1 cells, or in the presence of pentamidine 25 nM. Two independent experiments are shown. HA, haemagglutinin; tub, β -tubulin; CHX, cycloheximide; $\alpha\text{-HA}$, anti-HA serum. All data for these graphs are contained in **Figure 6—source data 1**.

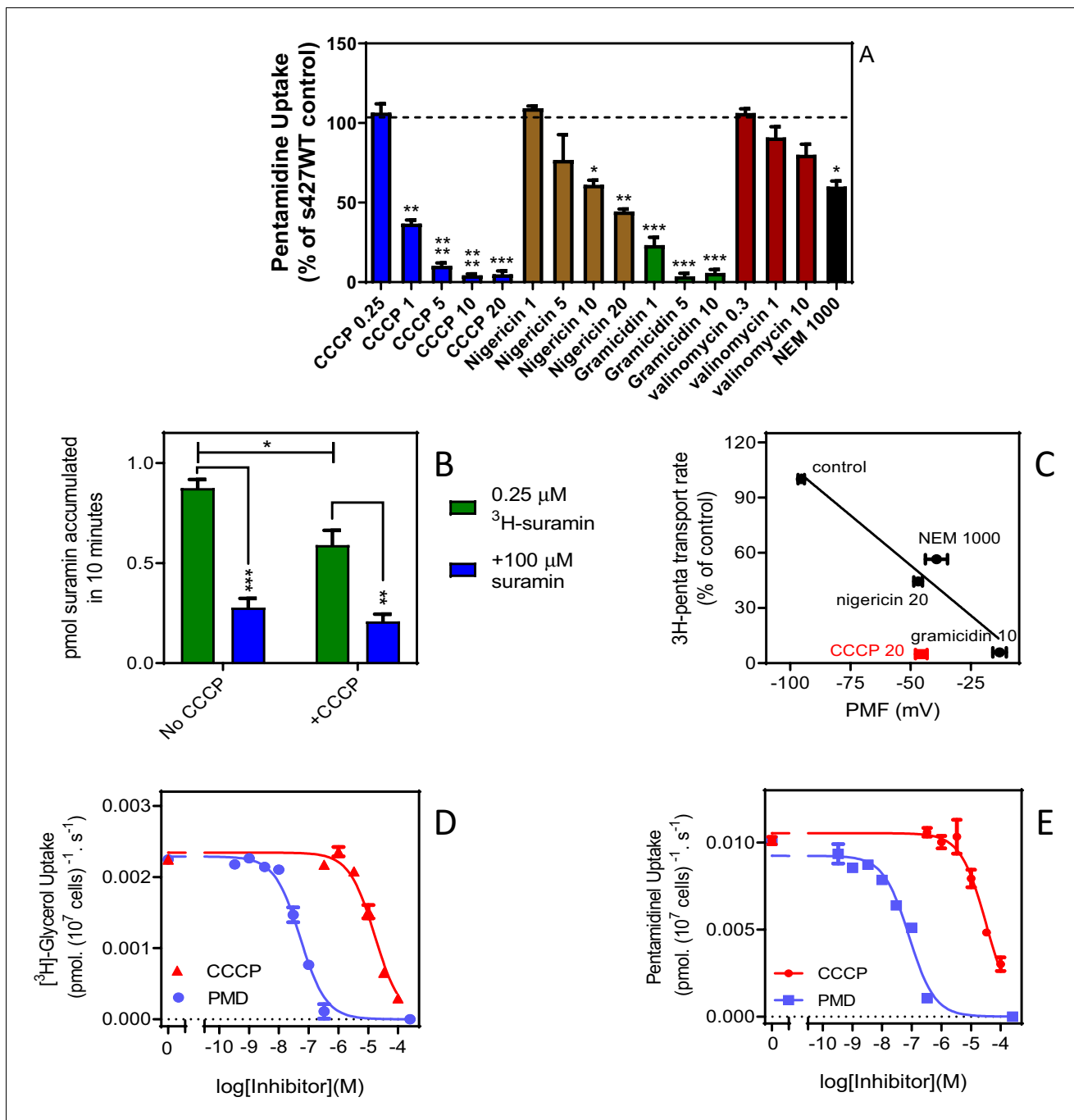


Figure 7. High affinity pentamidine uptake in *T. b. brucei* is sensitive to ionophores. (A) Uptake of 25 nM [³H]-pentamidine in s427WT bloodstream forms was measured in the presence of 1 mM adenosine to block the P2 transporter, and in the further presence of various ionophores at the indicated concentrations in μ M. Incubation with radiolabel was 5 min after a 3 min pre-incubation with ionophore. Accumulation of radiolabel was expressed as a percentage of the control, being a parallel incubation in the absence of any ionophore. Bars represent the average of 3–5 independent determinations (each performed in quadruplicate) and SEM. (B) Uptake of 0.25 μ M [³H]-suramin by *T. b. brucei* s427WT cells over 10 min. Cells were incubated in parallel, with or without the presence of 20 μ M CCCP (plus 3 min pre-incubation). Saturation of the suramin-receptor interaction was demonstrated by including 100 μ M unlabelled suramin (blue bars). Bars represent average and SEM or three independent experiments, each performed in quadruplicate. (C) Correlation plot of pentamidine transport rate versus protonmotive force (PMF), $r^2 = 0.93$, $p < 0.05$ by F-test. Concentrations in μ M are indicated in the frame. CCCP is shown in red and not included in the regression analysis. Each data point is the average of 4 or more independent repeats performed in quadruplicate. The values for PMF were taken from *de Koning and Jarvis, 1997b*. (D) Uptake of 0.25 μ M [³H]-glycerol by *aqp1/aqp2/aqp3* null cells expressing TbAQP2-WT. Dose response with CCCP and pentamidine (PMD), using an incubation time of 1 min. The graph shown was performed in triplicate and representative of three independent repeats. (E) As D but using 0.025 μ M [³H]-pentamidine and 30 s incubations.

Figure 7 continued on next page

Figure 7 continued

Representative graph in triplicate from three independent repeats. *, $p < 0.05$; **, $p < 0.01$; ***, $p < 0.001$ by Student's unpaired t-test. All data for these graphs are contained in **Figure 7—source data 1**.

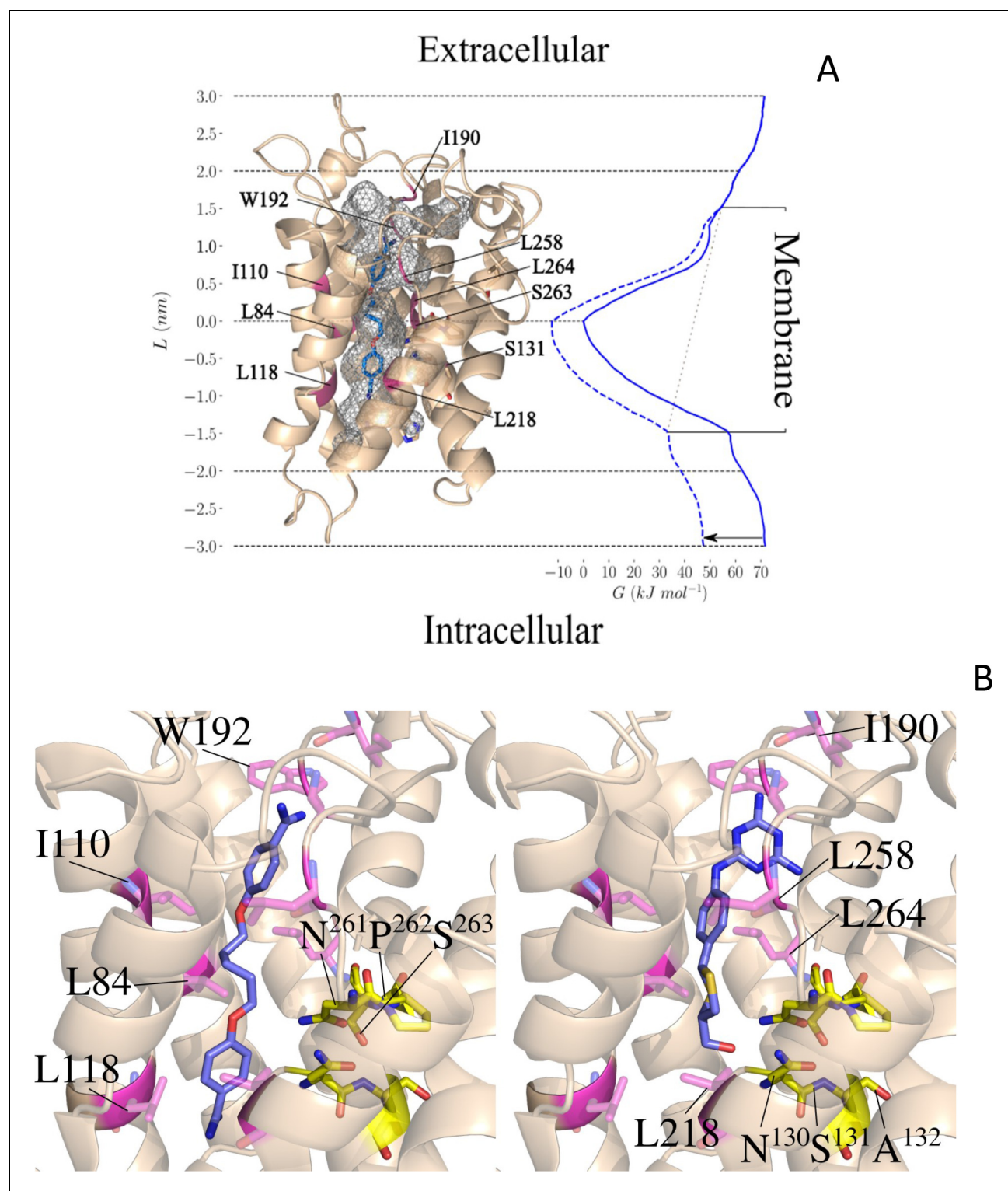


Figure 8. Pentamidine binding in TbAQP2 and free-energy profile of permeation (Left). (A) Docked conformation of pentamidine (blue) bound to the TbAQP2 (wheat). The protein and the ligand were modelled as described.⁴ The protein pore is shown in grey mesh, and the mutated positions described in the text are in magenta. (Right) Free-energy profile $G(L)$ (solid blue line) along the pore axis of TbAQP2 (L). The membrane voltage of *T. b. brucei* gives rise to a voltage drop across the membrane (gray dotted line), which alters the free-energy profile (dashed blue line includes V_m effect) and reduces the free-energy of pentamidine exit into the intracellular bulk by ~22 kJ/mol as compared to the extracellular side (black arrow). (B) Close-up views comparing the bound positions of pentamidine (left) and melarsoprol (right) and showing the mutated sites and major interactions with the AQP2 pore lining.

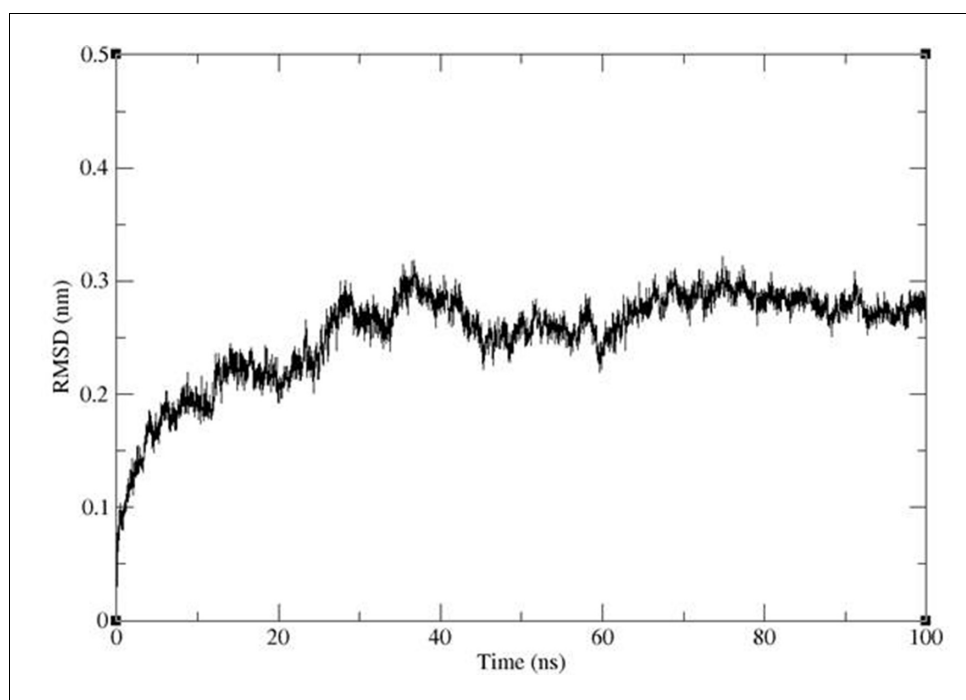


Figure 8—figure supplement 1. Backbone RMSD of the protein inserted into a lipid bilayer showing convergence to ~ 3 Å in a simulation of 100 ns length.

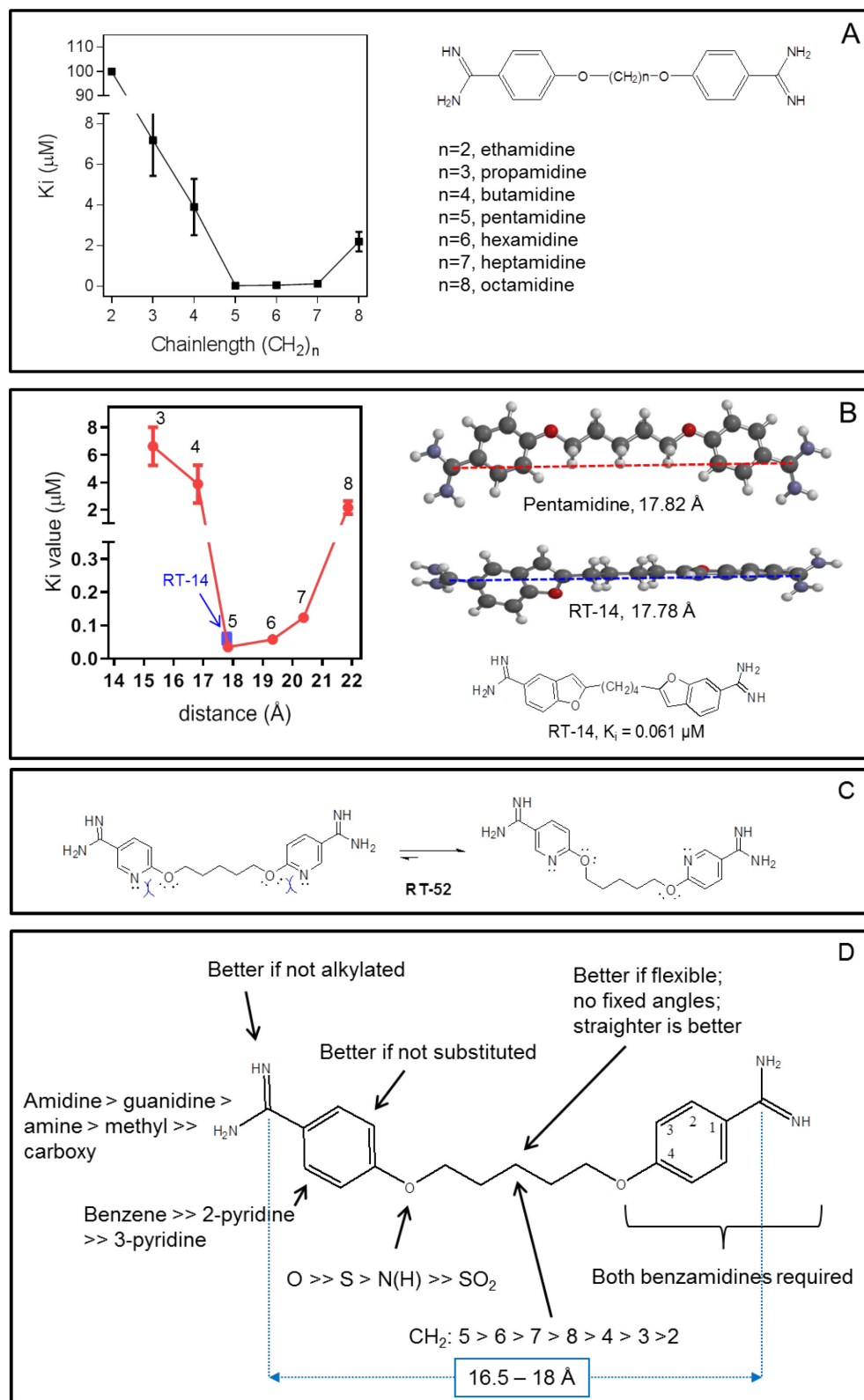


Figure 9. Correlation between linker chain length and affinity to HAPT1. (A) A series of pentamidine analogues with different methylene linker length was tested for inhibition of TbAQP2/HAPT1-mediated 25 nM [³H]-pentamidine transport (i.e. in the presence of adenosine to block the TbAT1/P2

Figure 9 continued on next page

Figure 9 continued

transporter). The K_i values are listed in **Table 1**. All K_i values are shown as average and SEM of 3 or more independent experiments, each performed in triplicate. (B) The distance between the amidine carbon atoms in the lowest-energy conformation was calculated using density functional theory as implemented in Spartan' 16 v2.0.7. Geometry optimisations were performed with the wB97XD functional and the 6–31G* basis set at the ground state in gas phase. Structures and distances shown represent the dication state that is overwhelmingly prevalent in aqueous solution at neutral pH. The numbered red data points correspond to the propamidine - octamidine series in frame A. (C) Repulsion between free electron pairs (double dots), indicated by curved blue lines for RT-52 in the *cis*-conformation, causing it to exist overwhelmingly in the *anti*-conformation. (D) Overview of SAR observations on the binding preferences of TbAQP2 for pentamidine and its analogues. All data for these graphs are contained in **Figure 9—source data 1**.

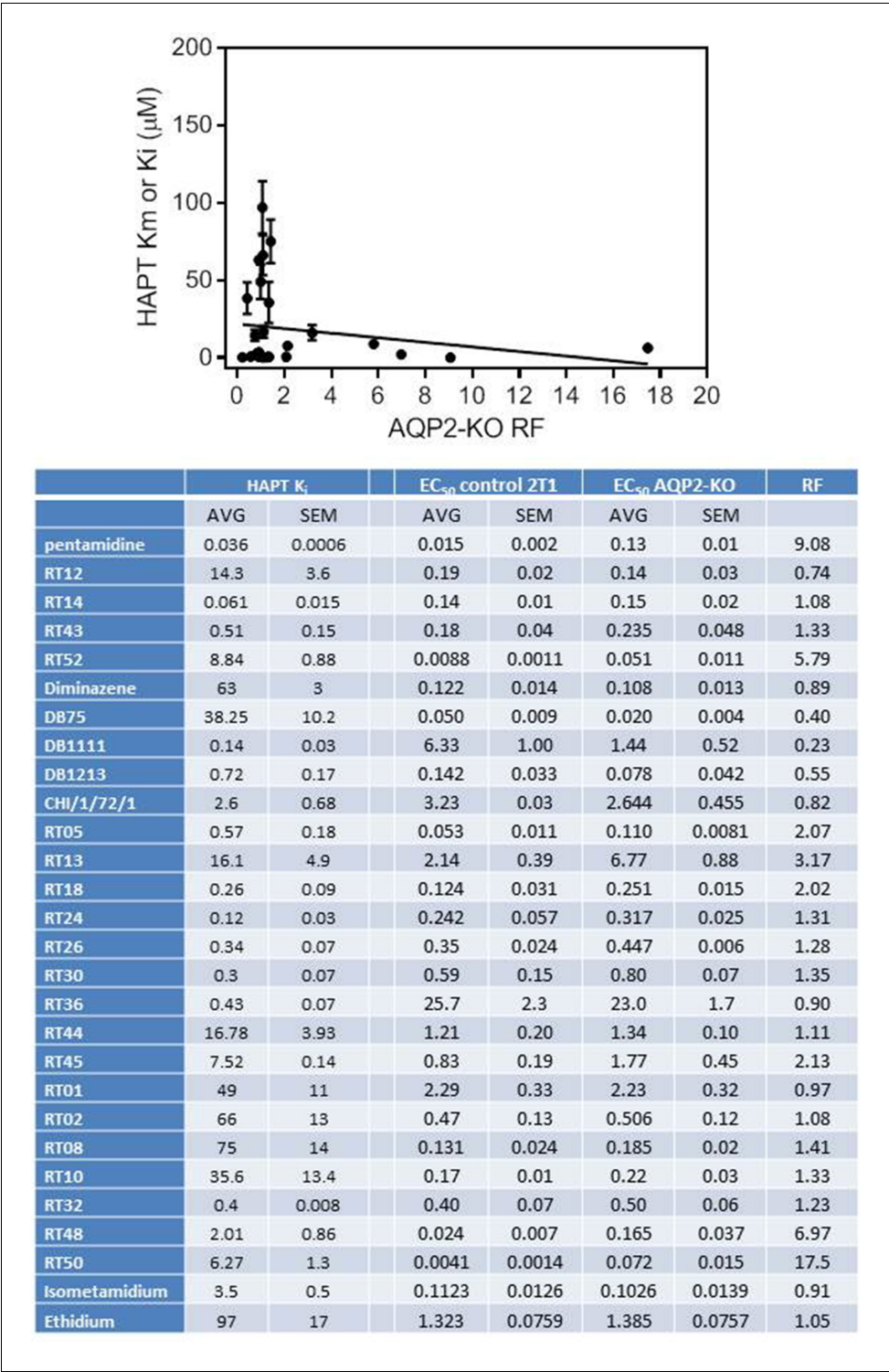


Figure 9—figure supplement 1. Correlation between the Resistance Factor (RF; $EC_{50}(\text{aqp2/3 null})/EC_{50}(\text{TbAQP2-WT})$) and the K_i value for inhibition of the High Affinity Pentamidine Transporter (HAPT1) encoded by TbAQP2. The pentamidine value (bold) is the K_m determined with radiolabeled pentamidine. The table lists the data points shown in the plot. The line was made by linear regression (Prism 6.0); correlation coefficient r^2 is 0.037. F-test: slope is not significantly different from zero ($p=0.33$). All values are in μM . All data for these graphs are contained in **Figure 9—source data 1**.